GUEST EDITORIAL

Earth and Planetary Physics
2: 439–443, 2018
doi: 10.26464/epp2018041

Introduction to special section on the China Seismo-Electromagnetic Satellite and initial results

XuHui Shen[1]*, Qiu-Gang Zong[2], and XueMin Zhang[3]*

[1]Institute of Crustal Dynamics, China Earthquake Administration, Beijing 100085, China;

[2]School of Earth and Space Science, Peking University, Beijing 100871, China;

[3]Institute of Earthquake Forecasting, China Earthquake Administration, Beijing 100036, China

Keywords: CSES satellite; scientific payload; data product; scientific application

Citation: Shen, X. H., Zong, Q-G., and Zhang, X. M. (2018). Introduction to special section on the China Seismo-Electromagnetic Satellite and initial results. *Earth Planet. Phys.*, *2*(6), 439–443. http://doi.org/10.26464/epp2018041

1. Introduction

The China Seismo-Electromagnetic Satellite (CSES), which is also called ZhangHeng-1 (ZH-1), is the first Chinese space-borne platform dedicated to geophysical field measurement and earthquake monitoring by detecting variations in the electromagnetic environment of space. The CSES was launched successfully at 15:51 on February 2, 2018, at China's Jiuquan Satellite Launching Center.

The CSES is a 3-axes-stabilized satellite, based on the Chinese CAST2000 platform, with a mass of about 730 kg and peak power consumption of about 900 W. Scientific data are transmitted in the X-Band at 120 Mbps. The orbit is circular Sun-synchronous, at an altitude of about 507 km, inclination of about 97.4°, descending node at 14:00 LT, and the designed life time is 5 years.

The main objectives of this mission are to monitor the near-Earth space environment and investigate possible electromagnetic perturbations related to natural disasters and human activities (Shen XH et al., 2018). The CSES can also be applied to study problems in many related fields, such as space physics, radio wave propagation, geophysics, and earthquake sciences.

The CSES orbit is strictly revisited each 5 days, so variations of the electromagnetic environment at the topside ionosphere can be monitored and compared every 5 days. All payloads are designed to work in the region within the latitude of ±65°. There are two operation modes for the CSES, survey and burst; the burst mode will be switched on automatically over all of China and the Circum-Pacific and Eurasia seismic belts.

The CSES has been equipped with eight scientific payloads, including a High Precision Magnetometer (HPM), an Electric Field Detector (EFD), a Search Coil Magnetometer (SCM), a Plasma Analyzer Package (PAP), a Langmuir Probe (LAP), a High Energetic

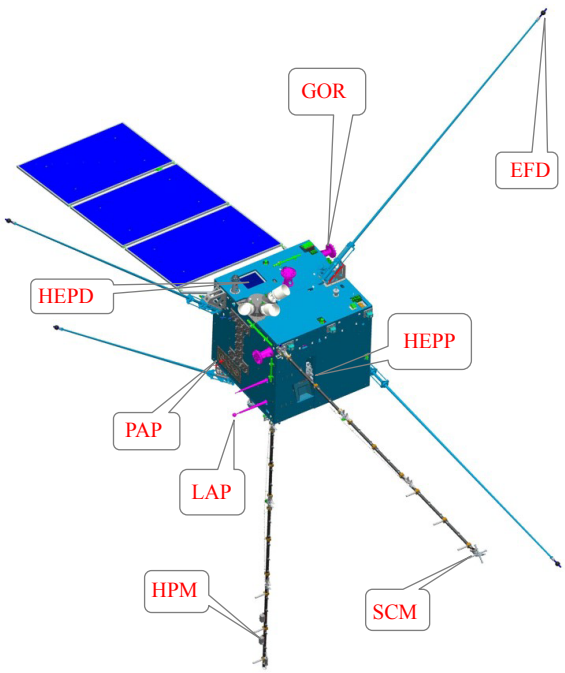

Figure 1. Shown is the CSES satellite. The CSES scientific payload includes: High-Energy Particle Detectors (HEPD) and the High-Energy Particle Package (HEPP) to measure energetic particle flux, energy spectrum, and type and direction of incident particles; a Search-Coil Magnetometer (SCM) and a High Precision Magnetometer (HPM) to measure the components and the total intensity of the magnetic field, respectively; a four-probe Electric Field Detector (EFD) to measure the electric field components in a wide range of frequencies; a Plasma analyzer Package (PAP) and a Langmuir probe (LAP) to measure plasma parameters; and a GNSS Occultation Receiver (GOR) and a Tri-Band Beacon to measure the density of electrons and to perform ionospheric tomography.

Correspondence to: X. H. Shen, shenxh@seis.ac.cn
X. M. Zhang, zhangxm96@126.com
Received 31 OCT 2018; Accepted 07 NOV 2018.
Accepted article online 13 NOV 2018.

Particle Package (HEPP) and High Energetic Particle Detector (HEPD), a GNSS Occultation Receiver (GOR) and a Tri-Band Beacon (TBB). Of these, the HEPD has been provided by the Italian National Institute of Nuclear Physic; the scalar detector of HPM was manufactured by the Austrian Space Institute. To minimize the effect of residual magnetism from the satellite platform, six booms connected with the four EFD sensors, one HPM sensor and one SCM sensor separately, are extended outside the satellite platform at a distance of 4.5 m (Figure 1).

Eight scientific payloads are used to measure the magnetic field (HPM), electromagnetic waves (EFD and SCM), *in-situ* plasma parameters (LAP and PAP), electron density profiles (GOR and TBB), and the energetic electron and proton spectrum (HEPP). Most of these payloads have been developed by China.

2. Satellite Ground Supply and Application System

The CSES mission consists of five systems the satellite platform, the launch vehicle, the launch site, the command and control system, and the ground supply and application system. The main tasks of the ground supply and application system are to make operation plans for the CSES satellite and its onboard payloads, to receive the scientific data, to produce high level data products, and to facilitate release of these data to the public.

Huang JP et al. (2018b) has presented an overall introduction to the CSES ground supply and application system managed by the Institute of Crustal Dynamics, China Earthquake Administration. The framework of the CSES ground supply and application system consists of four subsystems—an operation and control subsystem, a data management subsystem, a data processing subsystem, and a data service subsystem. All data sets from the 8 payloads will be processed and the data products will be made generally available.

CSES satellite data will be further divided into scientific data, remote sensing data, and auxiliary data. Each data set will be defined and described in detail, especially the scientific data. The data contents and format will be listed by filename. Registered users will find summary plots, how to access the data, and a user guider in the service subsystem.

The CSES application system has been working for more than 8 months since the CSES launch in February 2018. Scientific data sets accumulated during the commission phase have demonstrated that CSES instrumentation and supporting software are meeting designed requirements.

3. Initial Results from Scientific Payloads

3.1 Electromagnetic Type Payloads

The high precision magnetometer (HPM) contains two fluxgate sensors and a coupled dark state magnetometer (CDSM) to measure the scalar value and the vector of the Earth's magnetic field with a bandwidth from DC to 15 Hz (Cheng BJ et al., 2018). The two fluxgate (FGM) sensors are in a gradiometer configuration in order to reduce satellite interference.

In order to get clean vector magnetic field, several data processing and calibration methods have been adopted, including calibration of each sensor, absolute vector field correction, spacecraft magnetic interference elimination, and coordinate transformation (Cheng BJ et al., 2018).

Based on onboard measurement by HPM, Zhou B et al. (2018) introduced the main processing method, algorithm, and processing procedure. FGM and CDSM were first calibrated with the absolute vector magnetic field correction algorithm using CDSM data, and then the FGM linearity parameters were corrected according to the sensor calibration results on the ground. At the same time, ground test results verified that magnetic interference from the satellite platform had been eliminated. Finally, the transfer matrix between the FGM probe and star sensor was calibrated according to the characteristics of the magnetic field direction in low latitudes. The scientific data from HPM onboard CSES has been compared with measurements from SWARM satellites. Vector magnetic field measurements from the two satellites are in agreement with each other according to data from five continuous periods of geomagnetic quiet time.

The SCM on the CSES was manufactured by Beihang University, China; it is designed to measure the magnetic field fluctuation or electromagnetic waves in the low frequency range of 10 Hz–20 kHz (Cao JB et al., 2018). The SCM is comprised of a three-axis search coil sensor mounted on a 4.5 m boom. The orthogonality of the three axes of the search coil sensor mechanism is better than 0.13°. Three operational modes are included in the SCM—a survey mode, a burst mode over a specific area, and a calibration mode which produces standard signals at 625 Hz and 10 kHz.

In this special issue, Wang Q et al. (2018) present initial CSES SCM results. Four levels of data sets have been defined and described in detail. The data sets in different levels contain essentially three components of waveforms and spectra with the frequency of 10 Hz–20 kHz. SCM measurements have been further divided into three bands—ultra-low frequency band (10–200 Hz), extremely low frequency band (200-2200 Hz), and very low frequency band (1.8 kHz–20 kHz). Examples of data products for Level-2, Level-3, and Level-4 are presented. Level-4 data demonstrate that effects from man-made VLF transmitters can clearly be observed, and possible earthquake signals related to the August 5 event in Indonesia are analyzed and discussed.

The electric field detector (EFD) onboard CSES is designed to measure electric field fluctuations in the frequency range from DC to 3.5 MHz. Huang JP et al. (2018a) describe the EFD payload on ZH-1 and its preliminary results. The EFD consists of 4 sensor balls, each mounted on a 4.5 m boom outside the satellite, and an electronic box inside the satellite module.

EFD measurements are divided into 4 bands: ULF (DC-16 Hz), ELF (6 Hz–2.2 kHz), VLF (1.8 kHz–20 kHz), and HF (18 kHz–3.5 MHz). The sampling rates for each band are 125 Hz, 5 kHz, 50 kHz, and 10 MHz, respectively. There are two EFD working modes: survey and burst. For ULF, ELF, and HF, the sampling rates are the same for the two modes. For ULF and ELF, the waveforms of the electric field will be produced continuously. For the HF band, PSD data are produced every 2.048 s and the waveform data are recorded only at the beginning of every 0.002048 s. For VLF data, in the survey

mode, the PSD data are provided; in the burst mode, waveforms are provided.

Based on actual EFD observational results, the sensitivity of the EFD instrument is found to be 0.1 $\mu V{\cdot}m^{-1}{\cdot}Hz^{-\frac{1}{2}}$ (ULF), 0.05 $\mu V{\cdot}m^{-1}{\cdot}Hz^{-\frac{1}{2}}$ (10 Hz–20 kHz) and 0.1 $\mu V{\cdot}m^{-1}{\cdot}Hz^{-\frac{1}{2}}$ (20 kHz–3.5 MHz). The dynamic range of the EFD instrument is greater than 120 dB (DC-20 kHz) and 96 dB (20 kHz–3.5 MHz). These initial results demonstrate that the EFD on the CSES can satisfy the scientific objectives of CSES missions.

3.2 *In-situ* Plasma and Energetic Particle Measurements

The Langmuir probe (LAP) onboard the CSES has been designed for *in situ* measurements of the density and temperature of ionospheric electrons. Yan R et al. (2018a) present a brief description of the LAP and its initial results. Under the assumptions of an ideal plasma environment, they describe in detail the inversion analysis method of the I-V curve which is used, to obtain the final description of ionospheric electron density and temperature. The two LAP sensors are of different size, designed with different sweeping voltages under two working modes; the survey mode utilizes a 3 s sampling rate; in burst mode, the sampling rate is 1.5 s.

CSES measurements of ionospheric electron density (N_e) and temperature (T_e) based on data collected during the satellite's commission phase have been compared with DEMETER data sets. The spatial distribution of N_e/ T_e from these two satellite observations is essentially identical, which verifies that the LAP instrument onboard the CSES is working well. Furthermore, Yan R et al. (2018b) have conducted typical case studies for an earthquake and a magnetic storm event. They report that there are obvious changes before and after an earthquake or a magnetic storm, indicating that ionospheric parameters can be affected by an earthquake or a magnetic storm.

The HEPD particle detector was developed by the Italian LIMADOU (Ambrosi et al. 2018). The HEPD instrument uses a tower of scintillators and a silicon tracker to measure high energy electrons from 3 to 100 MeV and high energy protons from 30 to 200 MeV.

In this special issue, Chu W et al. (2018) introduce the high-energy particle package (HEPP) instrument developed by the Institute of High Energy Physics, CAS. The HEPP includes three independent detectors, HEPP-H, HEPP-L, and HEPP-X. HEPP-H and HEPP-L can detect, respectively, energetic electrons from 100 keV to 50 MeV and energetic protons from 2 Mev to 200 MeV. HEPP-X can measure the Solar X-ray flux in the low energy range 1 keV to 20 keV. The HEPP instrument is designed to measure energetic particles with high resolution (~10%), and high pitch angle resolution (~5°). Data products of the HEPP instrument have been described in detail; Level-2 data can be accessed by public users.

Comparison of data sets from the HEPD onboard the CSES with the ones from the NOAA POES satellite demonstrates that these two data sets agree with each other during quiet time periods. Further, HEPD data sets have been used to study the disturbance in radiation environments during a strong magnetic storm during August 25–27, 2018, with a minimum *Dst* of –174 nT.

3.3 Ionospheric Electron Profile Inversion

GNSS occultation receivers (GOR) have been used widely since the last century in satellite-based electron density profiling and ionospheric tomography, such as COSMIC, CHAMP, etc. since the last century. The GOR onboard the CSES, one of its eight scientific payloads, is configured for either precise satellite orbit determination or ionospheric parameter inversion (Lin J et al., 2018). Cheng Y et al. (2018) present and analyze CSES GOR results. The GOR instrument can receive the signals from both GPS and Beidou satellites, so it can obtain about 600 occultation events every day.

By comparison with 2 months of COSMIC data, N_mF_2 and h_mF_2 from CSES show the same global distribution features. Further, to validate data quality, three ground-based ionosonde stations located at low, middle, and high latitudes were selected for comparison. The RMS of N_mF_2 from the CSES GOR at the same region and same time period is about 9.41%, with correlation efficient larger than 0.87, while for h_mF_2 RMS is 7.8% and the correlation greater than 0.71.

Tri-Band Beacon (TBB) is installed on the CSES for the inversion of ionospheric structures. It consists of two systems, a transmitting system on the satellite and a receiver system on the ground. Three signals are transmitted, at f=150.012 MHz, 400.032 MHz, and 1066.752 MHz. Chen L et al. (2018) introduce the TBB's working principles, developed by the China Research Institute of Radio Wave Propagation. Unfortunately, the middle frequency about 400 MHz worked only for a few hours after launch of the CSES satellite.

Chen L et al. (2018) report examples of ionospheric inversion based on data from the two functioning frequency signals. Their results demonstrate that the equatorial ionospheric anomaly (EIA) could be seen; its north crest was located at ~20°.

4. Application

4.1 Earthquake Case Study

The CSES's main scientific objective is to monitor earthquake-related perturbations in the Earth's ionosphere. Since its launch in February, the CSES has detected several strong earthquakes with $M_s \geq 7.0$.

Yan R et al. (2018b) have analyzed unusual ionospheric signatures obtained from CSES prior to four different earthquakes—one with shallow depth (0–70 km), one with moderate depth (70–300 km) and two with deep focus (>300 km).

An *M*s 7.1 earthquake took place at Ile Hunter, Caledonia (21.95°S, 170.1°E), on August 29, 2018, at a depth of 20 km. The electron density (N_e) observed by the LAP onboard the CSES increased 12 and 9 days before the event in a region close to the epicenter.

As for other three earthquakes, CSES observations in ULF/ELF/VLF of electric field, electron density, oxygen ion density, proton flux, and ion drift velocity along the flying direction of satellite, have all been analyzed, and some perturbations possibly associated with earthquakes have been identified. These results illustrate that unusual electromagnetic wave features may relate to earthquakes. However, the earthquake-related phenomena were quite com-

plex. The seismo-ionospheric relationship requires further investigation.

4.2 Radio Wave Experiment

Another interesting topic is ionospheric disturbances caused by powerful radio waves from ground sources. *In situ* satellite observations can provide the information from the topside ionosphere, which promises to improve understanding of the mechanism between powerful ground-based radio waves and ionospheric perturbations.

In June 2018, for the first time, the SURA heating facility in Russia, together with the in-orbit CSES, carried out a series of experiments in emitting high frequency (HF) O-mode radio waves to disturb the ionosphere.

Zhang XM et al. (2018) report preliminary results related to those experiments, using CSES data sets. They analyze five cases, two cases observed in local daytime and three cases in local nighttime.

They observe that the pumping wave frequencies f_0 in the daytime were close to the critical frequency of the F_2 layer f_0F_2; however, no pumping waves were detected by the EFD instrument onboard CSES even when, on June 16, 2018, the emitted power reached 90 MW. Also, no obvious plasma disturbances were observed by CSES in those two daytime cases.

Among the three cases in local nighttime, pumping waves are clearly distinguished in the HF-band electric field at the emitted frequency when the emitted power was only 30 MW, and the power spectrum density of the electric field is found to be one order of magnitude larger than the normal background, with the propagating radius exceeding 200 km.

4.3 Particle Precipitation Induced by VLF Transmitters

The CSES mission aims also to study the existence of possible (temporal and spatial) correlations between ionosphere and magnetospheric perturbations as well as precipitation of particles from the inner Van Allen belts.

Satellite *in situ* observations have proved that ground-based VLF signals can penetrate into the topside ionosphere, even into the magnetosphere. Parrot et al. (2007) has presented the first observations of strong ionospheric perturbations generated by a powerful VLF ground-based transmitter.

As observed by the CSES, signals from ground-based VLF transmitters can be also distinguished easily in the space. In this special issue, Wang YL et al. (2018) report particle precipitation related to the VLF transmitter at NWC station located in Australia. The geometric characteristic of the electron precipitation caused by ground-based VLF transmitter NWC is analyzed quantitatively.

This new precipitation belt was located mainly to the east of the NWC station, longitude of 105° E–220° E (northern hemisphere) and 115° E–235° E (southern hemisphere) above the NWC source. The typical wisp structure is recorded along a single orbit, the L value ranging from 1.44 to 1.74, which very closely fits the L value of the NWC station (L~1.45). The maximum energy of the electrons emitted by the VLF transmitter was approximately 100–361.57 keV; the number of trapped electrons reached its maximum at 213.73 keV.

5. Summary

This special issue reports preliminary calibration data and new results obtained by the CSES. These papers address the scientific payloads onboard the CSES, their data products, and initial results related to earthquakes, magnetic storms, and wave-particle interactions.

The collaboration between the CNSA and the ASI have facilitated the successful inclusion of the HEPD onboard the CSES. During development of the CSES over the past 15 years, hundreds of scientists in China, France, Russia, Italy, Japan, the USA, etc. have contributed to this mission.

In closing, we are pleased to report that on September 13, 2018, the kick-off meeting of the CSES (02) satellite, which is expected to be launched in 2020, was hosted by the China Earthquake Administration. The launch of CSES (02) will create a two-satellite constellation.

Acknowledgments

This paper is supported by NSFC project (41674156). We gratefully acknowledge the power support of China National Space Administration and China Earthquake Administration, the sincere cooperation of Italian Space Agency and the hard work of all the developing team in the successful launch of the CSES.

References

Ambrosi, G., Bartocci, S., Basara, L., Battiston, R., Burger, W., …and Vitale, V. (2018). The HEPD particle detector of the CSES satellite mission for investigating seismo-associated perturbations of the Van Allen blets. *Sci China Tech Sci*, *61*, 643–652. https://doi.org/10.1007/s11431-018-9234-9

Cao, J. B., Zeng, L., Zhan, F., Wang, Z. G., Wang, Y., Chen, Y., Meng, Q. C., Ji, Z. Q., Wang, P. F., Liu, Z. W., and Ma, L. Y. (2018). The electromagnetic wave experiment for CSES mission: Search coil magnetometer. *Sci China Tech Sci*, *61*, 653–658. https://doi.org/10.1007/s11431-018-9241-7

Chen, L., Ou, M., Yuan, Y. P., Sun, F., Yu, X., and Zhen, W. M. (2018). Preliminary observation results of the Coherent Beacon System onboard the China Seismo-Electromagnetic Satellite-1. *Earth Planet. Phys.*, *2*(6), 505–514. https://doi.org/10.26464/epp2018049

Cheng, B. J., Zhou, B., Magnes, W., Lammegger, R., and Pollinger A. (2018). High precision magnetometer for geomagnetic exploration onboard of the China Siesmo-Electromagnetic Satellite. *Sci China Tech Sci*, *61*, 659–668. https://doi.org/10.1007/s11431-018-9247-6

Cheng, Y., Lin, J., Shen, X. H., Wan, X., Li, X. X., and Wang, W. J. (2018). Analysis of GNSS radio occultation data from satellite ZH- 01. *Earth Planet. Phys.*, *2*(6), 499–504. https://doi.org/10.26464/epp2018048

Chu, W., Huang, J. P., Shen, X. H., Wang, P., Li, X. Q., An, Z. H., Xu, Y. B., and Liang, X. H. (2018). Preliminary results of the High Energetic Particle Package onboard the China Seismo-Electromagnetic Satellite. *Earth Planet. Phys.*, *2*(6), 489–498. https://doi.org/10.26464/epp2018047

Huang, J. P., Lei, J. G., Li, S. X., Zeren, Z. M., Li, C., Zhu, X. H., and Yu, W. H. (2018a). The Electric Field Detector (EFD) onboard the ZH-1 satellite and first observational results. *Earth Planet. Phys.*, *2*(6), 469–478. https://doi.org/10.26464/epp2018045

Huang, J. P., Shen, X. H., Zhang, X. M., Lu, H. X., Tan, Q., and Wang, Q. (2018b). Application system and data description of the China Seismo-Electromagnetic Satellite. *Earth Planet. Phys.*, *2*(6), 444–454. https://doi.org/10.26464/epp2018042

Lin, J., Shen, X. H., Hu, L. C., Wang, L. W., and Zhu, F. Y. (2018). CSES GNSS ionospheric inversion technique, validation and error analysis. *Sci China Tech Sci*, *61*, 669–677. https://doi.org/10.1007/s11431-018-9245-6

Parrot, M., Sauvaud, J. A., Berthelier, J. J., and Lebreton J. P. (2007). First in-situ observations of strong ionospheric perturbations generated by a powerful VLF ground-based transmitter. *Geophys. Res. Lett.*, *34*, L11111. https://doi.org/10.1029/2007GL029368

Shen, X. H., Zhang, X., Yuan, S. G., Wang, L. W., Cao, J. B., Huang, J. P., Zhu, X. H., Piergiorgio, P., and Dai, J. P. (2018). The state-of-the-art of the China Seismo-Electromagnetic Satellite mission. *Sci China Tech Sci*, *61*, 634–642. https://doi.org/10.1007/s11431-018-9242-0

Wang, Q., Huang, J. P., Zhang, X. M., Shen, X. H., Yuan, S. G., Zeng, L., and Cao, J. B. (2018). China Seismo-Electromagnetic Satellite search coil magnetometer data and initial results. *Earth Planet. Phys.*, *2*(6), 462–468. https://doi.org/10.26464/epp2018044

Wang, Y. L., Zhang, X. M., and Shen, X. H. (2018). A study on the energetic electron precipitation observed by CSES. *Earth Planet. Phys.*, *2*(6), 538–547. https://doi.org/10.26464/epp2018052

Yan, R., Guan Y. B., Shen, X. H., Huang, J. P., Zhang, X. M., Liu, C., and Liu, D. P. (2018a). The Langmuir Probe onboard CSES: data inversion analysis method and first results. *Earth Planet. Phys.*, *2*(6), 479–488. https://doi.org/10.26464/epp2018046

Yan, R., Shen X. H., Huang, J. P., Wang, Q., Chu, W., Liu, D. P., Yang, Y. Y., Lu, H. X., and Xu, S. (2018b). Examples of unusual ionospheric observations by the CSES prior to earthquakes. *Earth Planet. Phys.*, *2*(6), 515–526. https://doi.org/10.26464/epp2018050

Zhang, X. M., Frolov, V., Zhao, S. F., Zhou, C., Wang, Y. L., Ryabov, A., and Zhai, D. L. (2018). The first joint experimental results between SURA and CSES. *Earth Planet. Phys.*, *2*(6), 527–537. https://doi.org/10.26464/epp2018051

Zhou, B., Yang, Y. Y., Zhang, Y. T., Gou, X. C., Cheng, B. J., Wang, J. D., and Li, L. (2018). Magnetic field data processing methods of the China Seismo-Electromagnetic Satellite. *Earth Planet. Phys.*, *2*(6), 455–461. https://doi.org/10.26464/epp2018043